Variable Delay Line for Phased-Array Antenna Based on a Chirped Fiber Grating

Beatriz Ortega, José L. Cruz, José Capmany, *Senior Member, IEEE*, Miguel V. Andrés, *Member, IEEE*, and Daniel Pastor, *Associate Member, IEEE*

***Abstract*—We present a theoretical and experimental analysis of the performance of phased-array antennas steered by a single chirped fiber grating. Two approaches consisting of conventional and single-sideband (SSB) modulation techniques of the optical signal are presented in order to compare their performance and suitability for beamforming applications in microwave antennas. By using a 40-cm-long chirped grating, we measure the phase and amplitude response and calculate the corresponding radiation patterns to demonstrate wide-band operation and continuous spatial scanning properties of both configurations. SSB modulation is presented as a real alternative to the first one offering broader operation band (4–18 GHz) for a given chirped grating and being less demanding on the fiber grating characteristics.**

***Index Terms*—Fiber gratings, microwave antenna, optical fibers, phased arrays, time-delay lines.**

I. Introduction

OPTICAL beamforming networks for phased-array antennas have been under intense research during the last decade [1]. Optical fiber is used in these systems to guide a given lightwave as a carrier for a microwave signal that drives every element of the antenna. The operation of wide-band phased arrays requires to keep the beampointing direction stable at different frequencies by using a true-time-delay line. There have been several proposals for wide-band operation during the last years, but recently, the use of fiber Bragg gratings in fabricating programmable delay lines has become of great importance in the development of optical beamforming networks for steering phased-array antennas.

In the first approaches, multiple beamforming networks were based on a number of uniform fiber Bragg gratings written at different positions on optical fibers and the distances between gratings determine the beampointing direction of the array antenna [2]–[5]. The optical carrier is routed to the antenna radiators by a wavelength division multiplexing (WDM) demultiplexer [6] or by a timing unit [7]. This system assures broad-band operation, but it only allows a discrete number of beampointing angles.

It has been demonstrated that chirped fiber gratings can produce a linear phase delay of the modulating signal at microwave frequencies and the slope of the phase response can be continuously modified by tuning the wavelength of the optical carrier [8]. Recently, a new delay line operating at a constant wavelength has been presented in order to simplify the optical beamforming network [9]. Therefore, they are a suitable beamformer for wide-band steering of phased-array antennas. By using an eight-element array, we showed a continuously tunable and stable beampointing angle in a frequency range of 2–6 GHz [10] and radiation patterns of a three-element array steered by two chirped gratings have been measured in the RF range (3–3.6 GHz) [11].

In this paper, we present theoretical and experimental results of the phase and amplitude distributions of a microwave modulating signal when the optical carrier is reflected by a chirped grating. Two modulation techniques, i.e., double-sideband (DSB) and single-sideband (SSB), have been used in simulations and experiments in order to compare the performance of each one of them. The radiation patterns of a 32-element array have been calculated from experimental data to demonstrate wide-band operation up to 18 GHz by using the SSB modulation technique.

The paper is structured as follows. DSB modulation and SSB modulation techniques are studied in Section II, showing the grating response when light is amplitude modulated at different RF frequencies throughout the microwave bands C–X–Ku (4–18 GHz).

Section III shows experimental measurements of a 4-nm-chirped grating response when an optical signal, which acts as a carrier, is amplitude modulated by a microwave signal using DSB and SSB modulation techniques. Amplitude and time-delay responses were measured within the range of operation of the grating in each case at several RF frequencies. Section IV presents computed radiation patterns of a 32-element antenna using the phase and amplitude distributions obtained experimentally from grating reflection under both modulating configurations showing wide-band operation. Wavelength spacing between different optical carriers are chosen in order to show continuous spatial scanning properties and maximum spatial range. Finally, Section V summarizes the main results and the conclusions of this paper.

Manuscript received April 22, 1999. This work was supported by the Dirección General de Ciencia y Tecnología of Spain under Grant TIC97-1153 and Grant TIC98-0346.

B. Ortega, J. Capmany, and D. Pastor are with the Departamento de Comunicaciones, Universidad Politécnica de Valencia, 46022 Valencia, Spain (e-mail: bortegat@dcom.upv.es).

J. L. Cruz and M. V. Andrés are with the Departamento de Física Aplicada, Universidad de Valencia, Burjassot 46100 Valencia, Spain.

Publisher Item Identifier S 0018-9480(00)06536-4.

II. Theoretical Analysis

A. DSB Modulation

Consider a microwave signal of frequency Ω amplitude modulating an optical carrier of frequency ω by a conventional DSB technique. The modulated lightwave is reflected by a fiber

grating of reflectivity $\boldsymbol{R}(\omega) = R(\omega)e^{j\Phi(\omega)}$ and the electric field at low modulation rates is a sum of terms

$$R(\omega)e^{j\omega t} \quad R(\omega-\Omega)e^{j(\omega-\Omega)t} \quad R(\omega+\Omega)e^{j(\omega+\Omega)t} \quad \text{c.c.} \tag{1}$$

After detection by a fast photodiode and provided higher order harmonics are negligible at low modulation rates, the time dependence of the electric field in the microwave transmission line can be expressed in the form

$$E(t) = E(\Omega, \omega)e^{j(\Omega t+\Psi(\Omega,\omega))} \tag{2}$$

where the amplitudes $E(\Omega, \omega)$ and phases $\Psi(\Omega, \omega)$ are as follows:

$$\begin{aligned} E(\Omega, \omega) = &\frac{1}{2}R(\omega) \\ &\cdot \big[(R(\omega+\Omega)\cos(\Phi(\omega+\Omega)-\Phi(\omega)) \\ &\quad + R(\omega-\Omega)\cos(\Phi(\omega)-\Phi(\omega-\Omega)))^2 \\ &\quad + (R(\omega+\Omega)\sin(\Phi(\omega+\Omega)-\Phi(\omega)) \\ &\quad + R(\omega-\Omega)\sin(\Phi(\omega)-\Phi(\omega-\Omega)))^2\big]^{1/2} \end{aligned} \tag{3}$$

and as shown in the equation at the bottom of this page.

If the modulation frequency is much smaller than the grating bandwidth, (3) can be approximated as

$$\begin{aligned} E(\Omega, \omega) &= |R(\omega)|^2 \\ \Psi(\Omega, \omega) &= \frac{\Phi(\omega+\Omega)-\Phi(\omega-\Omega)}{2}. \end{aligned} \tag{4}$$

Therefore, the phase of the RF signal, from (4) can be written as follows:

$$\Psi(\Omega, \omega) = -\tau(\omega)\cdot\Omega \tag{5}$$

where $\tau(\omega) = -(d\Phi(\omega)/d\omega)$ is the time delay of the fiber Bragg grating.

Hence, if the modulation frequency is low enough to preserve the linewidth of the optical carrier, the phase of the modulating signal is linear with the modulation frequency Ω and, therefore, the phase slope can be modified by changing the frequency ω of the optical carrier.

A set of wavelengths λ_i placed inside the bandpass grating will be reflected by the grating and used as optical carriers to drive the array elements; the wavelength that feeds every radiator is selected by using a tunable narrow-bandpass filter (bandwidth: BW $\sim 2f_{\max}$) (see Fig. 1). The corresponding amplitudes and phases arising from the reflection at the Bragg grating determine the radiation pattern of the array antenna. The far field of the array of N elements spaced by a distance d is given by the well-known expression [12]

$$AF(\theta) = \sum_{i=0}^{N-1} E_i(\Omega, \omega_i)e^{j(\Psi_i(\Omega,\omega_i)+i(\Omega/c)\,d\cdot\sin\theta)} \tag{6}$$

where $E_i(\Omega, \omega_i)$ and $\Psi_i(\Omega, \omega_i)$ are given by (3), c is the speed of light, and θ is the radiating angle.

The distance d between the antenna elements must be chosen to avoid the existence of more than one main lobe in the radiation pattern. The spacing criterion in terms of the maximum scan angle $\theta_{\max}$ is the following:

$$\frac{d}{\lambda_{\mathrm{RF}}} < \frac{1}{1+\sin\left(|\theta_{\max}|\right)} \tag{7}$$

where $\lambda_{\mathrm{RF}}$is the minimum microwave wavelength.

Provided (5) is satisfied—the modulation frequency is smaller than the grating bandwidth—the beampointing angle corresponding to the main lobe of the array antenna θ_0 can be expressed in terms of the grating time delay

$$\sin(\theta_0) = \frac{c}{d}\cdot\big[\tau(\omega_i)-\tau(\omega_{i-1})\big]. \tag{8}$$

Equation (8) states that the beampointing direction is not dependent on the RF frequency under the approximation mentioned above and, therefore, the grating is a true time-delay beamformer suitable for wide-band applications. The wavelengths of the optical carriers feeding the antenna elements determine the scan angle of the antenna, by means of the difference between corresponding time-delay values.

The time-delay τ of a fiber grating depends on the grating chirp. The function $\tau(\omega)$ is linear in gratings with a linear chirp; in that case, the beamforming network can operate by distributing a set of equally spaced optical frequencies to the array elements and the beampointing direction can be continuously controlled by the frequency step.

1) Results: Light of different optical wavelengths is amplitude modulated by a conventional technique (i.e., DSB), and after reflection in a linearly chirped Bragg grating, they are used to drive the elements of an array antenna. The signal should be distributed to the antenna elements through an $1 \times N$ power splitter and subsequently filtered by a set of N tunable bandpass filters, as it is illustrated in Fig. 1. The results of the simulation of every stage of this system are presented below.

The response of a fiber Bragg grating can be computed by using the forward-to-backward coupled-mode equations in an optical fiber, described in [13]. Fig. 2(top) shows the reflection coefficient and time-delay spectral response of the linearly chirped grating we have used in this theoretical study. Both of them are shown versus the normalized frequency deviation from

$$\Psi(\Omega, \omega) = \operatorname{arctg}\left[\frac{(R(\omega+\Omega)\sin(\Phi(\omega+\Omega)-\Phi(\omega))+R(\omega-\Omega)\sin(\Phi(\omega)-\Phi(\omega-\Omega)))}{(R(\omega+\Omega)\cos(\Phi(\omega+\Omega)-\Phi(\omega))+R(\omega-\Omega)\cos(\Phi(\omega)-\Phi(\omega-\Omega)))}\right]$$

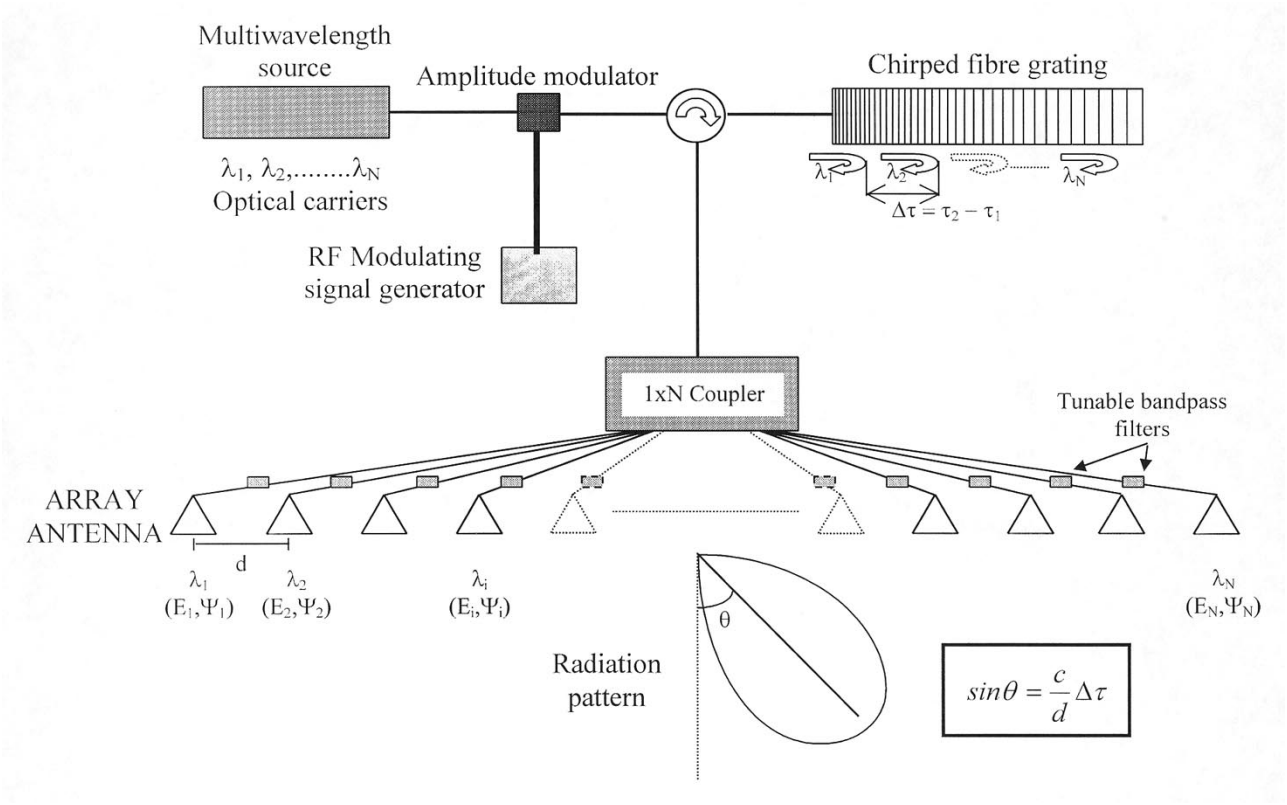

Fig. 1. Schematic of an array antenna steered by a chirped fiber grating. Different optical wavelengths are routed to the radiators through a WDM system.

the Bragg condition, $\delta L(\delta = (\omega - \omega_0)/v_g)$. The reflection characteristic shows a strong grating with a broad flat bandpass, corresponding to a 10-nm chirp at $\lambda_0 = 1550$ nm for a 10-cm-long grating, and the time-delay curve presents a linear component (slope of $\chi = 96$ ps/nm) with ripples along the bandpass. Note that total time delay of the grating, i.e., about 1000 ps, would be appropriate for steering a 32-element antenna in a 0°–90° spatial range with 18-GHz maximum frequency operation.

When light is amplitude modulated by a conventional DSB technique, the phase and amplitude of the microwave signal after reflection in the grating can be calculated by using (3) and (5). Fig. 2(upper middle)–(lower middle) show the amplitude—$E(\Omega, \omega)$—and time delay—$\tau(\omega) = -\Psi(\Omega, \omega)/\Omega$—of the modulated signal, reflected by the grating at modulation frequencies of 4, 11, and 18 GHz. The main effect of the DSB is a degradation of the amplitude response of the grating along the bandpass. In fact, a double-rippled characteristic appears in the reflection band. Assuming linear approximation, in such a strong grating, (3) becomes $E(\Omega, \omega) \approx \cos(\Delta\tau\Omega/4)$, where $\Delta\tau$ is the time-delay difference between both sidebands. The fast varying oscillation follows the rippled time-delay characteristic [see Fig. 2(top)], while the slow one corresponds to the modulating frequency term, whose period decreases as Ω increases.

However, the phase response of the grating improves when light is modulated. The original time delay of the grating [see Fig. 2(top)] has a strong rippled characteristic that disappears as a consequence of the RF modulation. Note that, at high modulation frequencies, the grating time delay exhibits a nearly perfect linear behavior.

In the modulation process, there are two signals arising from the beating between the optical carrier and each sidelobe (frequencies $\omega + \Omega$ and $\omega - \Omega$), which interfere in order to give the detected signal at the microwave modulating frequency. Within the bandpass, $\rho(\omega) \approx \rho(\omega + \Omega) \approx \rho(\omega - \Omega)$ and then from (3), $E(\omega, \Omega)$ drops to zero when the following condition is satisfied:

$$\theta(\omega + \Omega) - \theta(\omega) = \pi + \left[\theta(\omega) - \theta(\omega - \Omega)\right]. \tag{9}$$

Substituting the grating phase response $\theta(\omega)$ by the second-order Taylor series, we obtain that light drops to zero when time-delay difference between both sidebands is an integer value times the period of the RF signal, which corresponds to the following modulating frequency f_{null}:

$$f_{\text{null}} = \frac{1}{\lambda_0}\sqrt{\frac{c}{2\chi}}. \tag{10}$$

We can, therefore, establish a maximum operation frequency by setting the 3-dB dropping signal level respect to the nonmodulated one, which is found to be $f_{\max} = f_{\text{null}}/\sqrt{2}$. Therefore, beating between the two sidebands state a limitation of the RF frequency range. For a grating with $\chi = 96$ ps/nm, the maximum frequency is about 18 GHz.

The limitation arising from signals beating can be overcome by using an SSB technique modulation, as will be discussed in the following section.

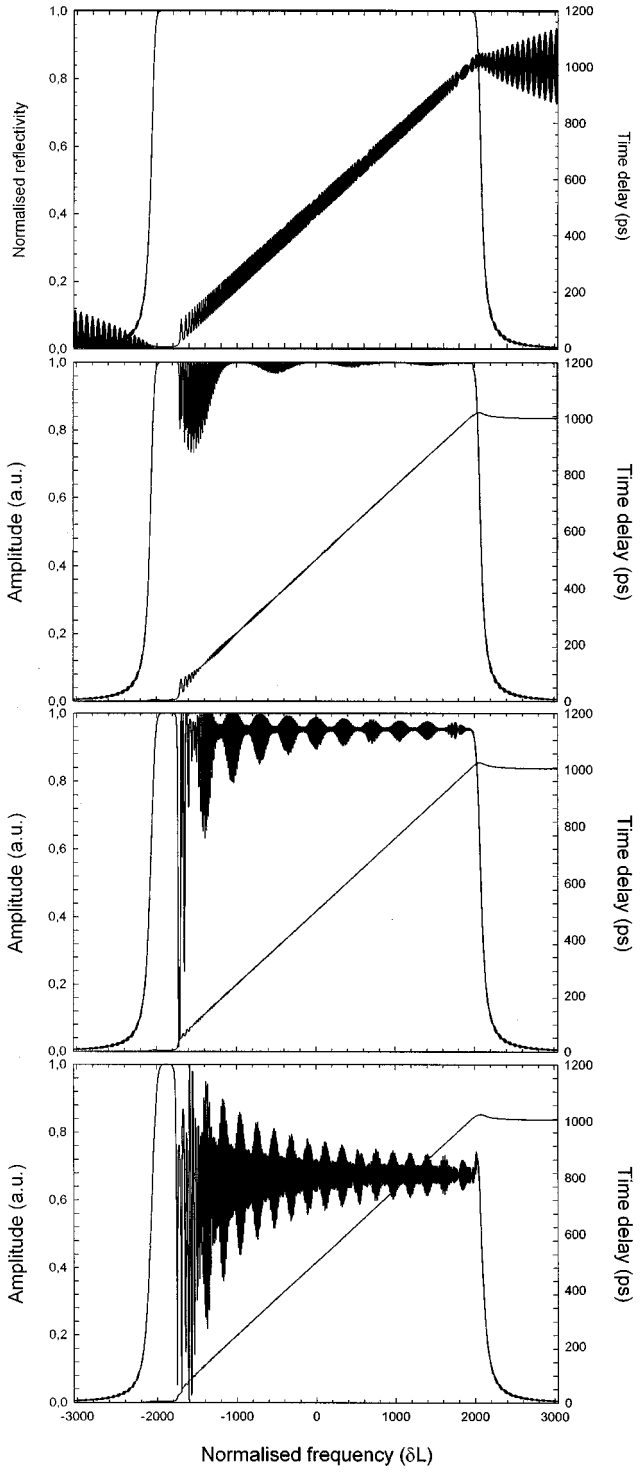

Fig. 2. Grating reflectivity and time-delay responses ($\chi = 96$ ps/nm). (top) Original response: when light is amplitude modulated by a conventional modulation technique at different RF frequencies. (upper middle) 4 GHz. (lower middle) 11 GHz. (bottom) 18 GHz.

B. SSB Modulation

In the previous section, we discussed about limitations in maximum microwave frequency operation arising from beating of both sidebands in conventional DSB modulation, which causes the cancellation of modulated light at certain RF frequency. However, this problem can be solved by using SSB modulation, which has been recently proposed as a high-resolution technique to measure the optical amplitude and phase response of fiber gratings [14]. In this technique, only one sideband is generated by the modulation process. Provided the lower sideband is suppressed, the electric field is a sum of terms

$$R(\omega)e^{j\omega t} \quad R(\omega+\Omega)e^{j(\omega+\Omega)t} \quad \text{c.c.} \tag{11}$$

(term with $\omega - \Omega$ instead of $\omega + \Omega$ will appear in (11) when the upper sideband is suppressed). The electric field has the same expression as (2) where the amplitude $E(\Omega, \omega)$ and phase $\Psi(\Omega, \omega)$ are the following:

$$\begin{aligned} E(\Omega, \omega) &= |R(\omega)| \cdot |R(\omega+\Omega)| \\ \Psi(\Omega, \omega) &= \Phi(\omega+\Omega) - \Phi(\omega) \end{aligned} \tag{12}$$

and (5) is also satisfied. By substituting amplitudes and phases given by (12), (6) will provide the far field of the array antenna in the same way as described in the previous section.

By using the SSB modulation technique, the amplitudes and phases of the modulated signal do not include any beating between two phase terms as happened in (3) for the DSB technique. Therefore, there is not any cancellation of the modulated signal when the SSB technique is employed, thus, theoretical limitation for high RF frequencies is not found.

1) Results: A Bragg grating with a varying spatial frequency of 2.5-nm chirp at 1550 nm for a nonapodised 10-cm-long grating was used in the theoretical study corresponding to the SSB-modulation technique. The reflectivity and time-delay responses of this grating are shown in Fig. 3(top), presenting a strong and flat reflection characteristic as well as a strongly linear component in the grating time-delay curve (slope of $\chi = 410$ ps/nm). Total time delay of the grating is designed to cover the 0°–90° spatial range for a 32-element antenna with a maximum operation frequency of 18 GHz. Note that, in the SSB configuration, total chirp is smaller because there are no limitations imposed on the time-delay slope [see (10)] arising from signal beating in the DSB technique.

Modulated light at several frequencies in the C–X–Ku range (4–18 GHz) is reflected by the grating, and which output contains the mapping of the optical carrier and the allowed sideband. The amplitude—$\varepsilon(\Omega, \omega)$—and time delay—$\tau(\omega) = -\Psi(\Omega, \omega)/\Omega$—of the reflected microwave signal are calculated by using (12), and results are shown in Fig. 3(middle) and (bottom), respectively, at RF frequencies of 4, 11, and 18 GHz. No rippling effects in the reflectivity or in the time delay appear due to the lack of phases beating. Also, responses at high RF modulation, i.e., 18 GHz, show the same quality as those of lower frequencies in order to drive the antenna elements.

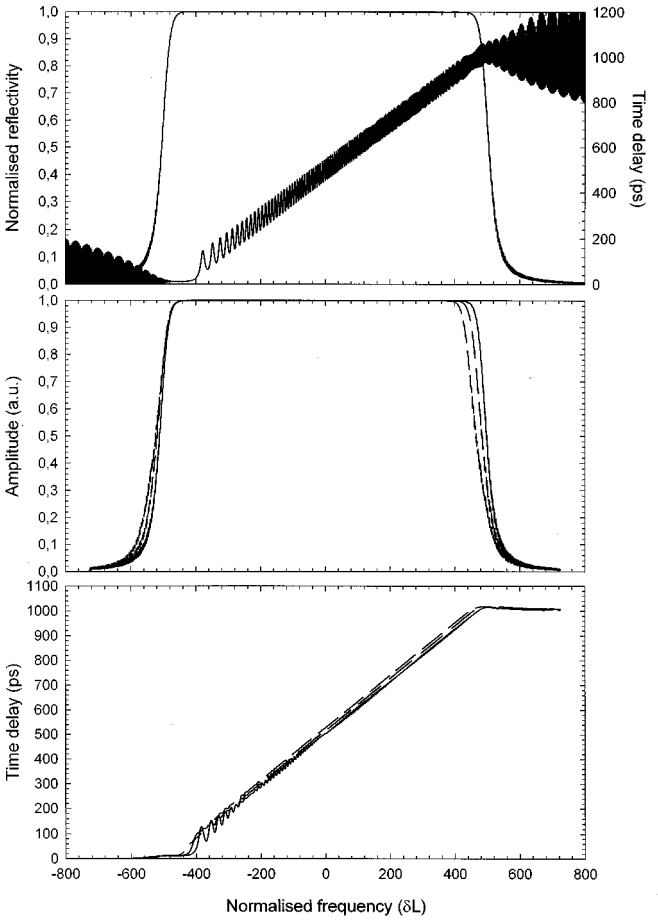

Fig. 3. Grating reflectivity and time-delay responses ($\chi = 410$ ps/nm). (top) Original response. Grating reflectivity (middle) and time-delay (bottom) responses when light is amplitude modulated by the SSB-modulation technique at different RF frequencies. (—) 4 GHz. (· · ·) 11 GHz. (- - -) 18 GHz.

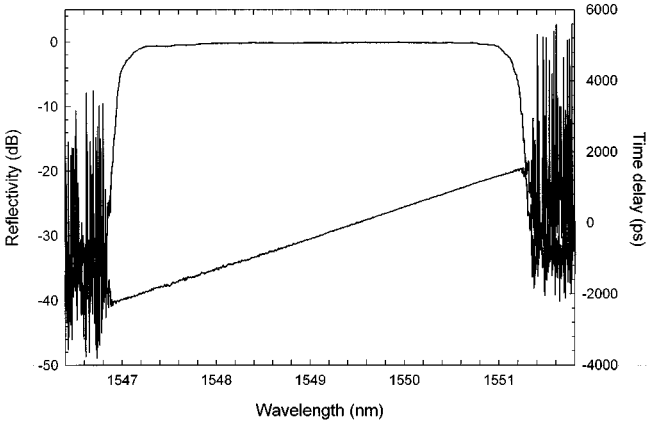

Fig. 4. Experimental measurements of the grating reflectivity and time-delay responses.

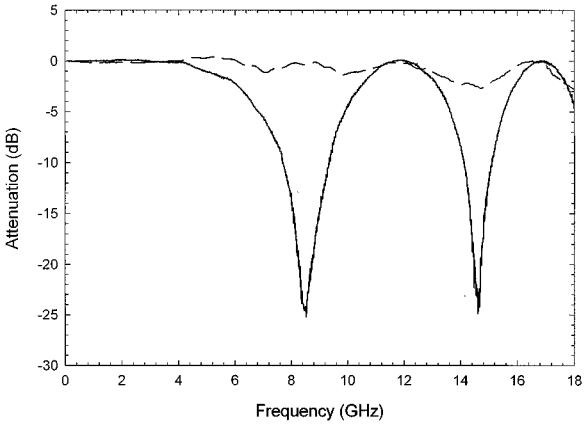

Fig. 5. Disperse attenuation of the modulated RF signal. (—) DSB technique. (· · ·) SSB technique.

III. Experimental Results

A 40-cm-long linearly chirped and apodised fiber grating was used in the experiment. The grating has a maximum reflectivity of 99.97% and 4-nm full-width at half-maximum (FWHM) bandwidth, with the time-delay dispersion slope of 835 ps/nm. Reflectivity spectra and time-delay characteristic show in Fig. 4 a uniform rejection band and linear delay curve. Measurement of reflectivity and time-delay response of the fiber grating was done by using the RF modulating technique of grating characterization [15] employing a low modulation frequency, i.e., 130 MHz, in order to guarantee modulation linewidth is much narrower than grating bandwidth and, therefore, provide correct measurements of the grating response.

The amplitude of the output light of a tunable laser is modulated by using an RF signal generated by a lightwave components analyzer (LCA) (HP8703A), which is also used in the signal detection. The modulated signal is launched into the fiber grating through a 3-dB coupler. After reflection, light goes back through the coupler to the fast detector of the optical components analyzer (OCA), which monitors the phase and amplitude of the RF signal. Corresponding measured amplitude and phase distributions at a given RF frequency are used in the calculation of radiation patterns of the array antenna.

A. DSB Modulation (DSB Technique)

In order to characterize the conventional RF modulation response of the grating, Fig. 5 (solid line) shows the reflectivity measurement when optical wavelength is set to the central one of the fiber grating, i.e., 1549 nm, and RF frequency is scanned in the 0.130–18-GHz range. The graph presents the attenuation of the signal strictly due to the effect of the presence of the grating in the system since modulator attenuation is corrected. Beating between both sidelobes generated in the modulation process produces a cancellation of the signal at 8.6 GHz [see (10)], being the characteristic frequency at the 3-dB signal level of 6.2 GHz. Therefore, the grating guarantees good operation of the system at RF frequencies lower than this value.

Spectral responses of the grating when light is modulated by a conventional technique at different microwave frequencies are presented in Fig. 6. Fig. 6 shows reflectivity and time-delay measurements using 2-, 4-, and 7-GHz signal modulation, respectively. Reflectivity characteristics are flat bandpass at 2 and

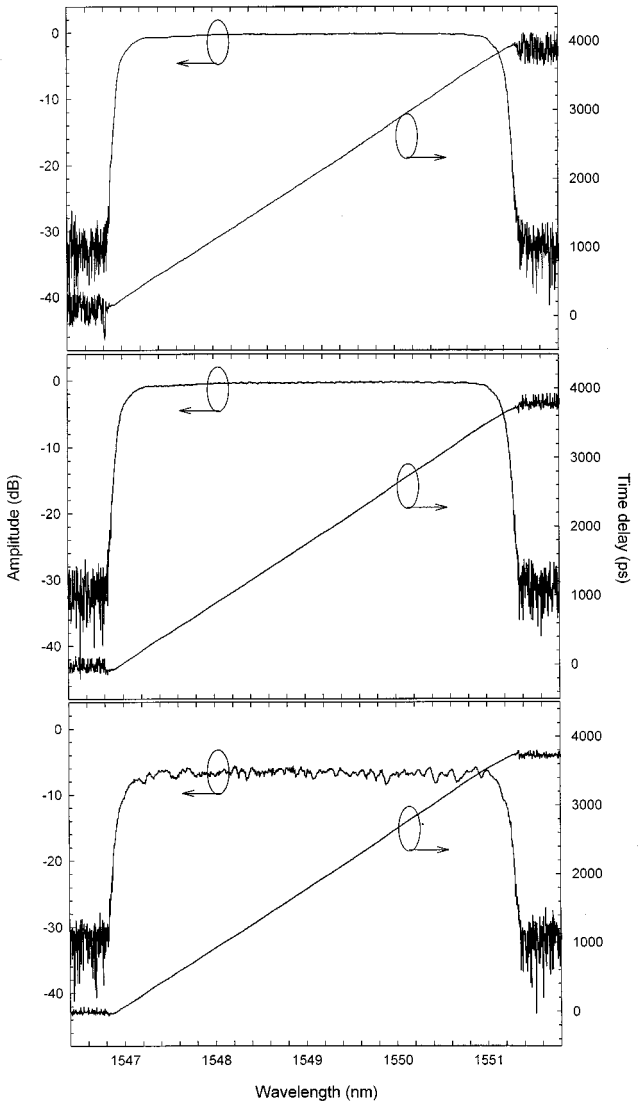

Fig. 6. Grating reflectivity and time-delay responses when light is amplitude modulated by a conventional modulation technique at different RF frequencies. (top) 2 GHz. (middle) 4 GHz. (bottom) 7 GHz.

4 GHz, but the spectra at 7 GHz is quite uneven due to the attenuation (see Fig. 5), which is 6 dB and, therefore, the response is not ideal. However, the time-delay response remains the same over the frequency range (2–7 GHz). The use of an apodised grating avoids the oscillating behavior in the amplitude response, previously shown as a consequence of the rippled characteristic in the original time delay (see Fig. 2).

B. SSB Modulation (SSB Technique)

A second experiment consisted on measurements of the grating response when light was modulated by the SSB technique. An RF modulator was used to suppress the upper sideband by means of two microwave driving signals 90° delayed by a microwave hybrid.

Optical wavelength was set to the central one in the grating bandpass, i.e., 1549 nm, and RF signal was scanning in the 0.130–18-GHz frequency range. Fig. 5 (dashed line) shows the

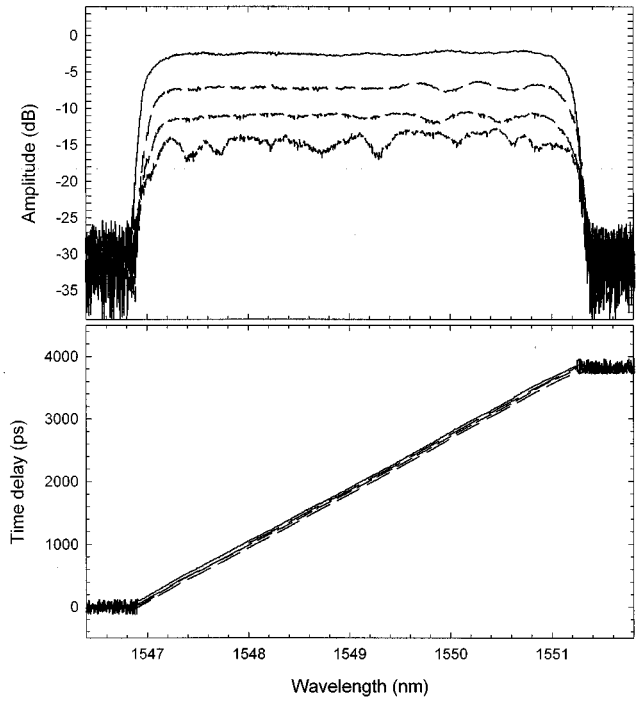

Fig. 7. Grating reflectivity (top) and time-delay (bottom) responses when light is amplitude modulated by the SSB modulation technique at different RF frequencies. (—) 4 GHz. (· · ·) 10 GHz. (· · ·) 15 GHz. (- · - · -) 18 GHz.

reflectivity response exhibiting the attenuation of the signal strictly due to the effect of the presence of the grating in the system, with a suppression of the notch that appeared by using DSB modulation. No intrinsic limitation in maximum RF frequency exists for the chirped grating.

Spectral response of the chirped grating when the optical signal is RF modulated at 4, 10, 15, and 18 GHz are presented in Fig. 7. Flat reflectivity characteristics are found in the grating response at 4-, 10-, and 15-GHz frequencies, although increasing attenuation of the modulator at high frequencies provokes a nonideal response at 18 GHz because of the increasing signal noise. Time-delay curves are linear and show the predicted behavior in previous section in all the frequency range (4–18 GHz). Broader band operation is demonstrated by using the SSB modulation technique with a single chirped grating since higher RF frequencies are in the operation range than in the previous section, in which a conventional modulation method was used.

IV. Radiation Patterns

Radiation patterns of a 32-element antenna have been calculated from the amplitude and phase distributions, measured in the previous section. Their experimental values are used as $E_i(\Omega, \omega_i)$ and $\Psi_i(\Omega, \omega_i)$, respectively, in (6) in order to calculate the array factor of the antenna. Spacing between radiator elements was set for a given maximum RF frequency following (7).

Using experimental values shown in Fig. 6 in a conventional modulation setup, and fixing elements spacing at $d = 21.4$ mm (corresponding to $\Omega_{\max} = 7$ GHz), calculated radiation patterns

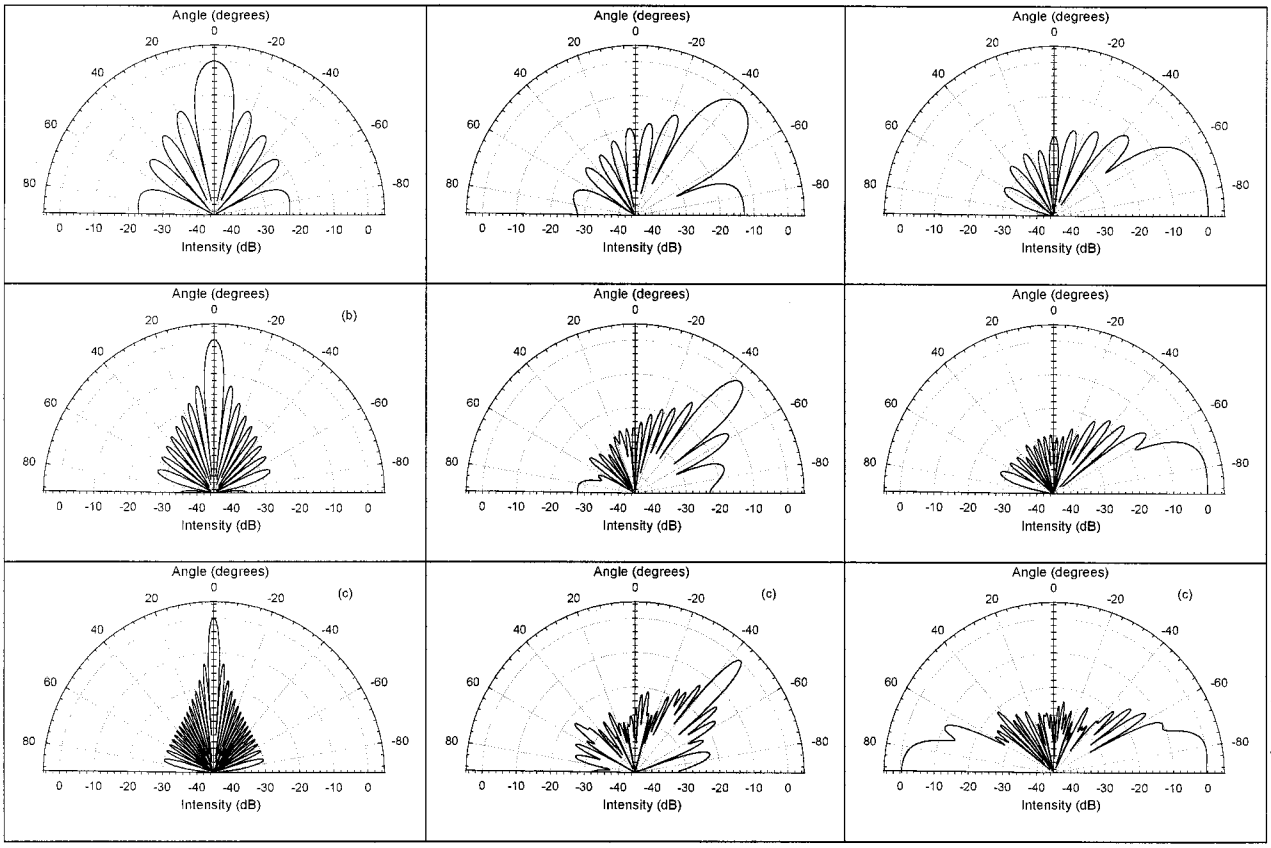

Fig. 8. DSB technique. Radiation patterns of a 32-element array antenna steered by a chirped grating. (top) 2 GHz. (middle) 4 GHz. (bottom) 7 GHz.

are shown in Fig. 8. Graphs corresponding to 2, 4, and 7 GHz are shown in Fig. 8, respectively. Every graph contains radiation patterns pointing at 0°, 43.6°, and 80°, and the narrower main lobe is shown for the higher microwave frequency. Beampointing direction is maintained over the microwave frequency range (2–7 GHz), which guarantees the operation along this RF band. The sidelobe level is, in general, close to that predicted by theory, i.e., 13 dB. Some small asymmetries in the 43.6° beampointing angle due to small irregularities in the time-delay response. Aside from this small effect, symmetrical features of the radiation patterns are generally good due to the strongly linear behavior of the phase response, i.e., time delay of the radiating elements (see Fig. 6). Beamwidths at 3 dB for the 43.6° beampointing direction are 15.5°, 7.7°, and 4.5°, in accord to those predicted by theory [12]: 15.5°, 7.7°, and 4.4° at 2, 4, and 7 GHz, respectively.

Amplitude and phase distributions obtained by using the SSB technique are also used to calculate the radiation patterns of a 32-element array antenna. In this case, there is no maximum frequency, thus, spacing between elements is set to provide correct performance at higher RF frequency, i.e., $d = 8.3$ mm ($\Omega_{\max} = 18$ GHz). In the same way as we did with calculations from DSB modulation measurements, Fig. 9 presents graphs corresponding to 4-, 10-, 15-, and 18-GHz frequencies, respectively, and every graph shows the radiation patterns pointing at 0°, 39°, and 70° directions. Broader band operation is demonstrated since the beampointing angle of the main lobe is maintained over the 4–18-GHz range. Beamwidths for the 39° beampointing direction are: 18.7°, 7.4°, 5.1° and 4.3°, coincident with theoretically predicted values [12].

However, in the 39° direction, the graphs present a strongly asymmetric component due to deviations of the time delay in respect to the linear one. Moreover, the uncertainty in the time-delays measurement now leads to larger relative time-delay error due to the fact that, in this case, the time-delay difference between two adjacent elements required for a given beampointing angle is smaller because we fixed a larger maximum operation frequency (18 GHz) than in the DSB setup (7 GHz).

V. Summary and Conclusions

In this paper, we have presented theoretical and experimental results of a chirped fiber grating beamformer when light is amplitude modulated by two different techniques. Conventional and SSB modulation techniques are shown to be valid for broad-band operation in phased-array antennas, where every element is driven by a different optical wavelength, in which amplitude and phase depends on the grating response. Spacing between optical carriers can be changed

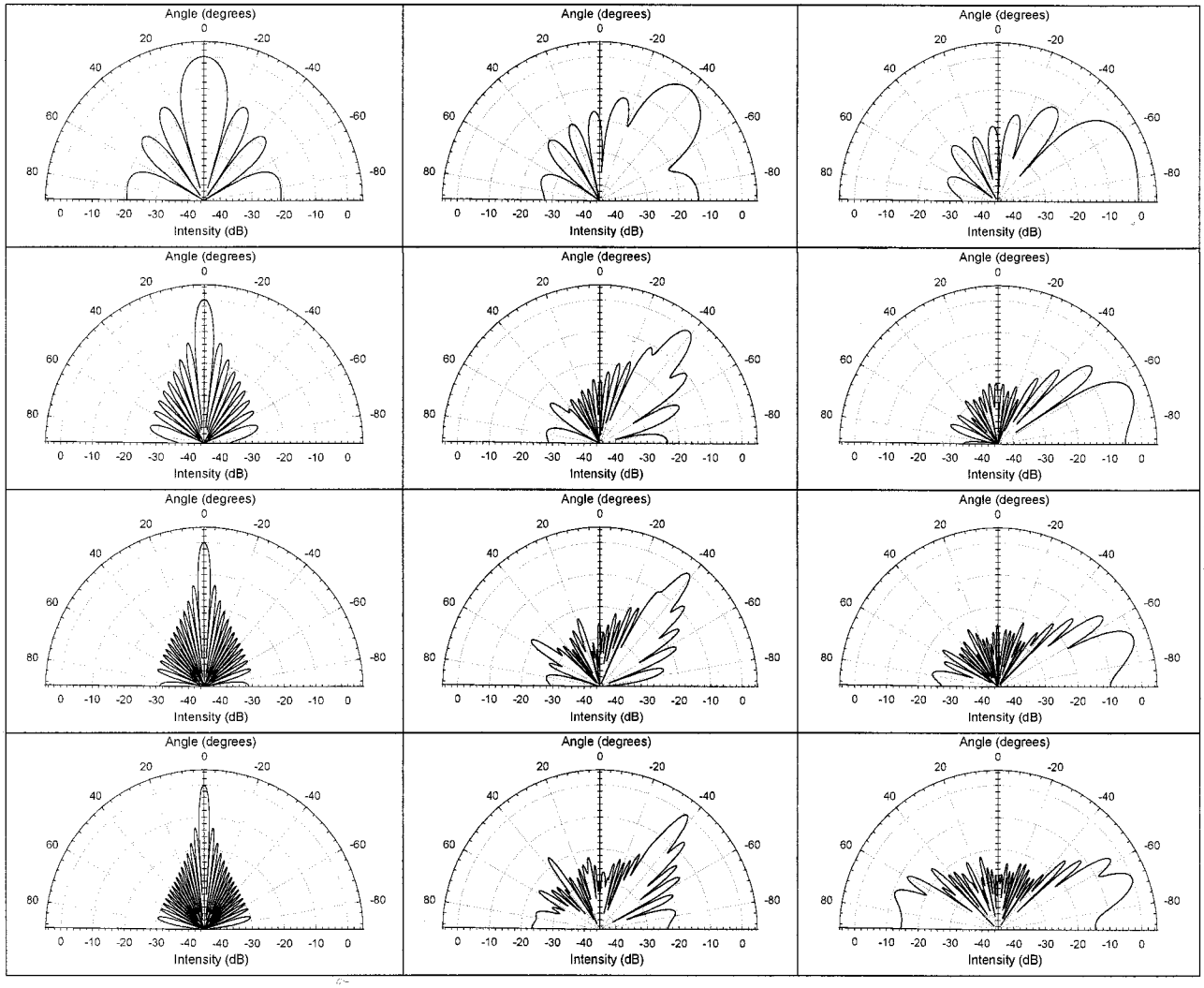

Fig. 9. SSB technique. Radiation patterns of a 32-element array antenna steered by a chirped grating. (top) 4 GHz. (upper middle) 10 GHz. (lower middle) 15 GHz. (bottom) 18 GHz.

continuously, as does the time delay between them, and both are compared in order to improve the antenna operation. As a conclusion, the SSB technique is proposed as an alternative to the first one, presenting no RF frequency limitations and showing higher performance.

High RF frequencies deteriorate the amplitude signal when DSB techniques are employed, while this is not relevant when an SSB technique is applied. On the contrary, time-delay responses improve their linear characteristic at higher frequencies for both modulation techniques.

Furthermore, the DSB technique is more restrictive about grating characteristics. The operation at 18-GHz maximum frequency imposes a limitation on the time-delay slope, and the chirp must be large enough, i.e., 10 nm, to provide the allocation of 32-element carriers spaced by the maximum δL value, which corresponds to 90° beampointing direction. Nevertheless, the SSB technique is less demanding, and a 2.5-nm linearly chirped grating can steer the 32-element antenna scanning along 90° at 18 GHz since no restrictions are imposed over a maximum time-delay slope.

REFERENCES

[1] I. Frigies and A. J. Seeds, "Optically generated true-time delay in phased array antennas," *IEEE Trans. Microwave Theory Tech.*, vol. 43, pp. 2378–2386, Sept. 1995.

[2] D. T. K. Tong and M. C. Wu, "Programmable dispersion matrix using fiber Bragg grating for optically controlled phase array antennas," *Electron. Lett.*, vol. 32, pp. 1532–1533, 1996.

[3] H. Zmuda, R. A. Soref, P. Payson, S. Jhons, and E. N. Toughlian, "Photonic beamformer for phased array antennas using a fiber grating prism," *IEEE Photon. Technol. Lett.*, vol. 9, pp. 241–243, Feb. 1997.

[4] G. A. Ball, W. H. Glenn, and W. W. Morey, "Programmable fiber optic delay line," *IEEE Photon. Technol. Lett.*, vol. 6, pp. 741–743, June 1994.

[5] A. Molony, C. Edge, and I. Bennion, "Fiber grating time delay for phased array antennas," *Electron. Lett.*, vol. 31, pp. 1485–1486, 1995.

[6] D. T. K. Tong and M. C, Wu, "A novel multiwavelength optically controlled phased array antenna with a programmable dispersion matrix," *IEEE Photon. Technol. Lett.*, vol. 8, pp. 812–814, June 1996.

[7] D. A. Cohen, Y. Chang, A. F. J. Levi, H. R. Fetterman, and I. L. Newberg, "Optically controlled serially fed phased array sensor," *IEEE Photon. Technol. Lett.*, vol. 8, pp. 1683–1685, Dec. 1996.
[8] J. L. Cruz, B. Ortega, M. V. Andrés, B. Gimeno, D. Pastor, J. Capmany, and L. Dong, "Chirped fiber Bragg gratings for phased array antennas," *Electron. Lett.*, vol. 33, pp. 545–546, 1997.
[9] B. Ortega, J. L. Cruz, M. V. Andrés, A. Díez, Pastor, and J. Capmany, "Microwave phase shifter based on a fiber Bragg grating operating at constant wavelength," in *Optical Fiber Conf. Tech. Dig.*, San Diego, CA, 1999, paper FK1.
[10] J. L. Cruz, B. Ortega, M. V. Andrés, B. Gimeno, J. Capmany, and L. Dong, "Array factor of a phased array antenna steered by a chirped fiber grating beamformer," *IEEE Photon. Technol. Lett.*, vol. 10, pp. 1153–1155, Aug. 1998.
[11] J. E. Román, M. Y. Frankel, P. J. Mattews, and R. D. Esman, "Time-steered array with a chirped grating beamformer," *Electron. Lett.*, vol. 33, pp. 652–653, 1997.
[12] C. A. Balanis, *Antenna Theory: Analysis and Design*. New York: Wiley, 1982, p. 222.
[13] T. Erdogan, "Fiber grating spectra," *J. Lightwave Technol.*, vol. 15, pp. 1277–1294, Aug. 1997.
[14] J. E. Román, Frankel, and R. D. Esman, "Spectral characterization of fiber gratings with high resolution," *Opt. Lett.*, vol. 23, pp. 939–941, 1998.
[15] D. Pastor, B. Ortega, J. Capmany, J. L. Cruz, J. Marti, M. V. Andres, M. J. Cole, and R. I. Laming, "Fully automatic simultaneous fiber grating amplitude and group delay characterization," *Microwave Opt. Technol. Lett.*, vol. 14, pp. 373–375, 1997.

Beatriz Ortega was born in Valencia, Spain, in 1972. She received the M.Sc. degree in physics from the Universidad de Valencia, Valencia, Spain, in 1995, and the Ph.D. degree in telecommunications engineering from the Universidad Politécnica de Valencia, Valencia, Spain, in 1999.

In 1996, she joined the Departamento de Comunicaciones, Universidad Politécnica de Valencia, where she was engaged with the Optical Communications Group and her research was mainly done in the field of fiber gratings. From 1997 to 1998, she was with the Optoelectronics Research Centre, University of Southampton, Southampton, U.K., where she was involved in several projects developing new add–drop filters or twin-core fiber-based filters. She is currently a Lecturer of the telecommunications engineering. She has authored or co–authored over 40 papers and conference contributions in fiber Bragg gratings, microwave photonics, and fiber filters. Her main interests include fiber-gratings applications, optical delay lines, and optical networks.

Dr. Ortega is a member of the Optical Society of America (OSA).

José L. Cruz was born in Cuenca, Spain, in 1964, He the Ph.D degree in physics from the University of Valencia, Valencia, Spain, in 1992.

His career initially focused on microwave devices for radar applications. He then was involved with the development of photosensitive optical fibers at the Optoelectronics Research Centre, University of Southampton, Southampton, U.K. He is currently a Professor Titular in the Department of Applied Physics, University of Valencia, where he conducts research on microwave photonics and fiber sensors.

José Capmany (S'88–M'91–SM'96) was born in Madrid, Spain, on December 15 1962. He received the Ingeniero de Telecomunicación and Ph.D. degrees from the Universidad Politécnica de Madrid, Madrid, Spain, in 1987 and 1991, respectively.

From 1988 to 1991, he was a Research Assistant in the Departamento de Tecnologfa Fotónica, Universidad Politécnica de Madrid. In 1991, he joined the Departamento de Comunicaciones, Universidad Politécnica de Valencia, where he began the activities on optical communications and photonics, founding the Optical Communications Group (http://www.gco.upv.es). He was an Associate Professor (1992–1996) and since 1996 has been a Full Professor in optical communications, systems and networks. In parallel, he has been the Telecommunications Engineering Faculty Vice-Dean (1991–1996) and Deputy Head of the Communications Department since 1996. His research activities and interests cover a wide range of subjects related to optical communications, including optical signal processing, fiber resonators, fiber gratings, RF filters, subcarrier multiplexing (SCM) and wavelength division multiplexing (WDM), and CDMA transmission, wavelength conversion, and optical bistability. He has authored or co-authored over 120 papers in international refereed journals and conferences. He has been a member of the Technical Program Committees of the European Conference on Optical Communications (ECOC), the Optical Fiber Conference (OFC), the Integrated Optics and Optical Communications Conference (IOOC), CLEO Europe, and the Optoelectronics and Communications Conference (OECC). He is an Editorial Board member of *Fiber and Integrated Optics*, *Microwave and Optical Technology Letters*, and the *International Journal of Optoelectronics*.

Prof. Capmany has also carried activities related to professional bodies and is the Founder and current Chairman of the IEEE Lasers and Electro-Optics Society (LEOS) Spanish Chapter and a Fellow of the Institution of Electrical Engineers (IEE), U.K. He was the recipient of the 1992 Extraordinary Doctorate Prize presented by the Universidad Politécnica de Madrid.

Miguel V. Andrés (M'91) was born in Valencia, Spain, in 1957. He received the Licenciado en Fisica degree and the Doctor en Fisica (Ph.D.) degree from the Universidad de Valencia, Valencia, Spain, in 1979 and 1985, respectively.

Since 1983, he has served successively as Assistant Professor and Lecturer in the Departamento de Fisica Aplicada, Universidad de Valencia. From 1984 to 1987, he was a Research Fellow with the Department of Physics, University of Surrey, Surrey, U.K. Until 1984, he was engaged in research on microwave surface waveguides. His current research interests are optical-fiber devices and systems for signal processing and sensor applications, and waveguide theory.

Dr. Andrés is a member of the Optical Society of America (OSA) and the Institute of Physics (IOP).

Daniel Pastor (S'95–A'97) was born in Elda, Spain, on November 5, 1969. He received the Ingeniero de Telecomunicacion and the Doctor Ingeniero de Telecomunicacion (Ph.D.) degrees from the Universidad Politécnica de Valencia, Valencia, Spain, in 1993 and 1996, respectively.

In 1993, he joined the Departamento de Comunicaciones, Universidad Politécnica de Valencia, where he was engaged in research with the Optical Communications Group. From 1994 to 1998, he was a Lecturer with the Telecommunications Engineering Faculty and became an Associate Professor in 1999. He has authored or co-authored over 45 papers and conference contributions in the fields of optical delay line filters, fiber Bragg gratings, microwave photonics, WDM and SCM lightwave systems. His current technical interests include microwave photonics, fiber Bragg grating applications, and V-RDM networks.